Journal Pre-proofs

Sorbent coatings for solid-phase microextraction targeted towards the analysis of death-related polar analytes coupled to comprehensive two-dimensional gas chromatography: Comparison of zwitterionic polymeric ionic liquids *versus* commercial coatings

Íris R. Carriço, Jéssica Marques, Maria J. Trujillo-Rodriguez, Jared L. Anderson, Sílvia M. Rocha

PII: S0026-265X(20)31612-X
DOI: https://doi.org/10.1016/j.microc.2020.105243
Reference: MICROC 105243

To appear in: *Microchemical Journal*

Received Date: 11 May 2020
Revised Date: 29 June 2020
Accepted Date: 30 June 2020

Please cite this article as: I.R. Carriço, J. Marques, M.J. Trujillo-Rodriguez, J.L. Anderson, S.M. Rocha, Sorbent coatings for solid-phase microextraction targeted towards the analysis of death-related polar analytes coupled to comprehensive two-dimensional gas chromatography: Comparison of zwitterionic polymeric ionic liquids *versus* commercial coatings, *Microchemical Journal* (2020), doi: https://doi.org/10.1016/j.microc.2020.105243

Sorbent coatings for solid-phase microextraction targeted towards the analysis of death-related polar analytes coupled to comprehensive two-dimensional gas chromatography: Comparison of zwitterionic polymeric ionic liquids *versus* commercial coatings

Íris R. Carriço[1], Jéssica Marques[2], Maria J. Trujillo-Rodriguez[3], Jared L. Anderson[3], Sílvia M. Rocha[2,*]

[1]*Faculty of Medicine, University of Porto, Alameda Professor Hernâni Monteiro, 4200-319 Porto, Portugal*
[2]*Departament of Chemistry &QOPNA/LAQV-REQUIMTE, Campus de Santiago, University of Aveiro, 3810-193 Aveiro, Portugal*
[3]*Department of Chemistry, Iowa State University, Ames, Iowa 50011 USA*

* Corresponding author. Tel. + 351 234401524; Fax + 351 234370084
E-mail address: smrocha@ua.pt (Sílvia M. Rocha)

ABSTRACT

Decomposition of bodies generates several types of polar volatile organic compounds (VOCs), whose types, patterns and ratios change during the various stages of decomposition and, therefore, their determination has huge potential to provide useful information to disclose events related to the time of death, or body surrounding environment. As sample preparation is a mandatory key-point in a method development, this research aims to develop a simple, accurate and rapid approach to study death-related polar VOCs based on headspace solid-phase microextraction (HS-SPME) combined with comprehensive two-dimensional gas chromatography-time of flight mass spectrometry (GC×GC-ToFMS) analysis. The performance of zwitterionic PIL-based fibers (containing a [$VIm^{+}C_{9}COO^{-}$] monomer and a [$(VIm)_2C1_2^{2+}$]-$2Br^{-}$ crosslinker), tailored for polar compounds, was evaluated for a set of 19 analytes associated with the unique odour created by decomposing bodies, and it was compared to the commercially-available fibers: divinylbenzene/carboxen/poly(dimethylsiloxane) – DVB/CAR/PDMS, poly(dimethylsiloxane)/divinylbenzene – PDMS/DVB and polyacrylate (PA). Fibers with absorptive-type mechanism, such as PA and PIL, showed the best results in the balance of the parameters studied, being able to detect analytes at ng level and providing a profile representative of the headspace composition, thus they may represent a useful tool to respond to current challenges in forensic taphonomy. The reproducibility (with relative standard deviation lower than 18 %, depending on the analyte) and relative recoveries (higher than 99.1 %) were similar and acceptable for both fibers. The zwitterionic PIL, with *ca*. 4 times smaller film thickness than PA, still has potential to have the best performance, supported by the efforts to obtain thicker sorbent coatings.

Keywords:

comprehensive two-dimensional gas chromatography
death-related analytes
polar analytes
zwitterionic polymeric ionic liquids
solid phase microextraction

1. Introduction

Forensic taphonomy studies post-mortem changes of human remains by extraction of information from decomposed and skeletonised bodies. It focuses largely on environmental effects – including decomposition (in soil and water) and interaction with organisms (plants, insects and other animals). Events close to the time of death, events that happened at the time of death, and events in the immediate or long-term period after death are studied. Forensic taphonomy provides a wide scope for forensic investigations by analysing processes that affect the preservation, observation and recovery of dead bodies and enables the reconstruction of their biology or ecology and the circumstances of their death [1,2]. A very important part of the taphonomy studies is the estimation of the post-mortem interval (PMI), since it helps determine the time in which a specific incident happened, assessing whether the suspects were able of committing a crime or not. There are many methods currently used to estimate PMI, such as corpse, algor mortis – decrease of the body temperature –, rigor mortis – body rigidity characterized by stiffening of the limbs –, livor mortis – settling of blood in the lower portion of the body –, corneal opacity and the chemical composition of the vitreous humour [3,4]. However, most of these methods are either empirical or very subjective and are only useful in the early post-mortem period. For this reason, other ways of estimating PMI have been developed, including the measurement of physical changes, biochemical components, DNA or RNA degradation, and forensic entomology – study of the invasion of arthropods (including insects, myriapods, arachnids and crustaceans) and their developmental stages found in decomposing bodies. Nevertheless, estimation of PMI is still a challenge in forensic science and new methods of determining it are needed [4,5].

During the decomposition process of a body, amino acids, carbohydrates and fatty acids are degraded, leading to the production and release of various volatile organic compounds (VOCs). In early decomposition, the metabolic changes are associated with energy metabolism and DNA still being synthesized. Afterwards, decay begins by the activity of endogenous enzymes and, finally, microorganisms interact with the body to continue the decaying process [6,7]. During decay initiated by endogenous enzymes, the families of VOCs produced are aldehydes, acids, sulfur-containing compounds and ketones [7]. During the decay initiated by the interaction of microorganisms with the body, acids, aldehydes, ketones, alcohols, esters, sulfur-containing compounds and nitrogen-containing compounds may be produced [7]. Therefore, the families of VOCs produced and released, due to the decomposition of the body, are all of the aforementioned compounds followed at a later stage by furans [6–14]. The types,

patterns and ratios of VOCs released change during the various stages of decomposition and, therefore, their determination has the potential of being used to estimate PMI [15–17]. Several research studies investigated VOCs released from body decomposition using headspace extraction with Tenax or Carbotrap®/Carbopack™ adsorbents, followed by thermal desorption and gas chromatography-mass spectrometry (GC-MS) [14,16,18,19] or, more recently, comprehensive two-dimensional gas chromatography coupled to time of flight mass spectrometry (GC×GC-ToFMS) [14,15,20]. However, the majority of these analysis only provided qualitative information about the presence/absence of certain compounds, frequency of detection and/or relative abundance in area. Advances in PMI estimation, reconstruction of overall death-odor profile, as well as their interaction with the surrounding environment requires the development of an effective analytical tool capable of collecting, separating, identifying, and also quantifying the analytes released by a cadaver during decomposition.

Furthermore, an inconvenience persists when performing these studies using headspace extraction/desorption since a desorption unit is necessary, which is not always available in chromatographic laboratories and its acquisition represents an extra cost [21,22]. An alternative to perform the sampling and extraction/desorption of VOCs consists in employing solid phase microextraction (SPME). SPME does not require expensive instrumentation and, at the same time, the technique fulfils the necessary requirements for implementation of green chemistry principles in analytical laboratories [23,24]. This solvent-free technique consolidates sampling, extraction, preconcentration and sample introduction into one step and exhibits reliability in terms of the enrichment capacity, as well as sensitivity and selectivity. It can be easily automated by coupling to instrumentation such as gas and liquid chromatographs with robotic or flow injection technologies. Further miniaturization of SPME may be possible, and the technique could be used as a direct sample introduction device for portable mass spectrometers as such systems are highly desirable for *in situ* analysis, which is particularly interesting in the forensic field [25].

Despite being one of the most well-established extraction techniques for volatile and semi-volatile compounds, SPME has not been extensively utilized to study body decomposition VOCs. Few studies have utilized in these analysis the commercially available poly(dimethylsiloxane)/divinylbenzene – PDMS/DVB [26–28], and divinylbenzene/carboxen/poly(dimethylsiloxane) – DVB/CAR/PDMS [29] sorbent coatings for SPME in combination with GC-MS. Furthermore, there are other SPME fibers that could be useful for the determination of polar VOCs related to body decomposition, fibers that include the commercially available polyacrylate (PA), and polymeric ionic liquids (PILs) [30]. PILs are

prepared by the polymerization of ionic liquid (IL) monomers. They possess low to negligible vapour pressure at room temperature and are highly chemically and mechanically stable. Very recently, PIL-based sorbent coatings comprised of zwitterionic IL monomers and dicationic IL crosslinkers have been developed for determining highly polar compounds such as short chain fatty acids [31].

The optimization of sample preparation parameters and the selection of the most suitable instrumental method are two fundamental steps in the construction of an analysis workflow, in order to provide high-quality data that may be useful to disclose events related to the time of death, or body surrounding environment, among others. Thus, the aim of this research was to develop a simple, accurate and rapid approach based on headspace (HS)-SPME combined with GC×GC-ToFMS to study polar VOCs released using headspace conditions that mimic the odor of body decomposition. With this objective, a set of 19 polar analytes associated with the unique odor created by decomposing bodies [15,16] were selected to implement the GC×GC-ToFMS experimental parameters. This sample mixture also served to compare the performance of PIL-based sorbent coatings (generated by the co-polymerization of the 1-vinyl-3-(nonanocarboxylate)imidazolium zwitterionic IL monomer – [$VIm^{+}C_{9}COO^{-}$] – and the 1,12-di(3-vinylimidazolium)dodecane bromide dicationic IL crosslinker – [$(VIm)_2C_{12}^{2+}$]2[Br^{-}] –) and commercial sorbent coatings (PDMS/DVB, DVB/CAR/PDMS and PA). The sorbent coating comparison was made based on extraction efficiency, reproducibility and representativeness of headspace composition.

2. Material and Methods

2.1. Chemical standards and materials

2.1.1. Commercial standards and SPME coatings

The following nineteen chemical standards were tested: dimethyl disulfide (≥99%), 3-methyl-1-butanol (99%), 1-hexanol (98%), 1-pentanol (≥99%), phenylethyl alcohol (99%), 3-octanol (99%), pentanoic acid (99%), 3-octanone (≥98%), *N*,*N*-dibutyl formamide (99%), 2,6-dimethyl pyrazine (98%), benzaldehyde (≥99%), hexanoic acid (99.5%), 2-acetylfuran (99%) and 2-hexen-1-ol (96%) were purchased from Sigma-Aldrich, Steinheim, Germany; butanoic acid, ethyl ester (≥99.5%) and benzyl alcohol (≥99%) were purchased from Fluka, Steinheim, Germany; *N*,*N*-dimethyl formamide (≥99.8% - Riedel-de-Haen, Seelze, Germany); 2,3-heptanedione (≥97% - Alfa Aesar, Kandel, Germany); and 2,4-pentanedione (99.8% - J. T.

Baker, Phillipsburg, NJ, USA). The list of analytes and their general chemical information are shown in **Table 1**.

Insert Table 1

Stock solutions of each of the standards in ethanol were prepared with concentrations of 5000 mg L^{-1}. Working solutions containing a mixture of the 19 analytes, with concentrations varying between 50 and 150 mg L^{-1}, were prepared by dilution of the stock solutions in ethanol. The standards with a concentration of 50 mg L^{-1} were dimethyl disulfide, 3-octanone, 2,6-dimethyl pyrazine, benzaldehyde, 2-acetylfuran, butanoic acid, ethyl ester, 2,3-heptanedione, and 2,4-pentanedione; those with 100 mg L^{-1}were pentanoic acid and hexanoic acid; those with 150 mg L^{-1} were 3-methyl-1-butanol, 1-hexanol, 1-pentanol, phenylethyl alcohol, 3-octanol, *N*,*N*-dibutyl formamide, *N*,*N*-dimethyl formamide, and 2-hexen-1-ol.

A SPME holder for manual sampling and the commercial sorbent coatings were purchased from Supelco (Bellefonte, PA, USA). The SPME coatings included PA (85 µm thickness), PDMS/DVB (65 µm), and DVB/CAR/PDMS (50/30 µm) StableFlex™ fibers, all with 1 cm of length. The following section describes the preparation of the zwitterionic PIL coating.

2.1.2. Preparation of zwitterionic PIL fiber

The zwitterionic IL (ZIL) monomer ($[VIm^{+}C_{9}COO^{-}]$) and an IL crosslinker ($[(VIm)_{2}C_{12}^{2+}]2[Br^{-}]$) employed for the preparation of the zwitterionic PIL sorbent coating were prepared according to previous methods [32–34] (details in Supplementary data, **Procedure S1**), using 1-vinylimidazole (≥99%), 1,12-dibromododecane (98%), or 10-bromodecanoic acid (95%), which were acquired from Sigma-Aldrich. For IL purification, Amberlite IRN78 hydroxide form, and the solvents acetonitrile, methanol, ethyl acetate, diethyl ether and tetrahydrofuran (ACS reagent grade) were also obtained from Sigma-Aldrich.

Insert Fig. 1

The zwitterionic PIL sorbent coating was prepared by *on fiber* UV co-polymerization of a mixture of the ZIL and IL crosslinker using DAROCUR 1173 as a free radical initiator. Prior to polymerization, the nitinol (Confluent Medical Technologies, Fremont, CA, USA) wire used as solid support was functionalized according to a previously reported method [35]. The wires were immersed in hydrogen peroxide (30%, w/w, Fisher Scientific) to impart hydroxyl groups

on the surface. The nitinol wires were then treated with vinyltrimethoxysilane (VTMS, Sigma-Aldrich) to functionalize the surface with vinyl moieties that facilitate anchoring the PIL to the solid support. The derivatized nitinol wires were then glued onto a commercial black SPME assembly and 1.3 cm were exposed for its coating. The co-polymerization was accomplished using a mixture consisting of the ZIL monomer and IL crosslinker (at a mass ratio of 1:1) together with DAROCUR 1173 (5% w/w respect to the ZIL monomer). The mixture was placed on the surface of the functionalized nitinol and the fibers were exposed to UV irradiation using a RPR-100 reactor with a spinning carousel (Southern New England Ultraviolet Company, Bradford, CT, USA). Co-polymerization was carried out at 254 nm for 2 h.

2.2. Headspace solid-phase microextraction conditions

The working solution (50 µL) was placed into a 25 mL vial (that was heated at *ca*. 30°C) in order to promote volatilization of the analytes aiming to mimic a headspace situation. The vial was capped with a polytetrafluoroethylene septum and a screw cap (Chromacol, Hertfordshire, UK) and placed in a thermostated bath adjusted to 30°C±0.1. The SPME fiber was inserted in the headspace for 20 min. Three independent aliquots of each sample were analysed. In order to avoid any cross-over contamination due to the sorbent coating, blanks, corresponding to the analysis of the fiber not submitted to any extraction procedure, were run between sets of three analyses.

Four SPME sorbent coatings were tested: DVB/CAR/PDMS (50/30 µm), PDMS/DVB (65 µm), PA (85 µm) and zwitterionic PIL (18 ± 6 µm) [31], all of 1 cm of length. Prior to use, the three commercial SPME fibers were conditioned at 250 °C for 30 to 60 min, according to the manufacturer's recommendations, and the zwitterionic PIL was conditioned at 175 °C for 30 min, as previously established [31]. All of the fibers were also conditioned daily for 10 min at their recommended temperature (250 °C or 175 °C).

Based on extraction efficiency, reproducibility and representativeness of headspace composition, the coatings with the best performance were selected and the analytical figures of the HS-SPME/GC×GC-TOFMS were determined under the selected desorption conditions and with concentrations of the analytes ranging from 50 to 3750 ng/vial.

2.3. GC×GC–ToFMS conditions for determination of polar analytes

After the extraction/preconcentration step, the SPME coating was manually introduced into the GC×GC–ToFMS injection port of the LECO Pegasus 4D instrument (LECO, St. Joseph, MI,

USA). Different desorption times (60 and 180 s) and temperatures (175 °C and 250 °C) were tested to prevent the degradation of the zwitterionic PIL and to guarantee quantitative desorption of the analytes from the fibers while avoiding *carry over*. The GC×GC–ToFMS system consisted of an Agilent GC 7890A gas chromatograph with a dual stage jet cryogenic modulator (licensed from Zoex), a secondary oven, and mass spectrometer equipped with a ToF mass analyser. The injection port was lined with a 0.75 mm I.D. splitless glass liner. Splitless injection mode was used. A Carbowax/BTR column (30 m × 0.25 mm I.D., 0.25 µm film thickness, J&W Scientific Inc., Folsom, CA, USA) was used as the ^{1}D (primary) column and an Equity 5 (0.79 m × 0.25 mm I.D., 0.25 µm film thickness, J&W Scientific Inc., Folsom, CA, USA) was used as a ^{2}D (secondary) column. The carrier gas was helium at a constant flow rate of 2.50 mL/min. The primary oven temperature program was as follows: initial temperature 40 ºC (hold 1 min), raised to 150 ºC (6 ºC min^{-1}) (hold 2 min), and then to 280 ºC (50 ºC min^{-1}). The secondary oven temperature program was 5 ºC offset above the primary oven. Both the MS transfer line and MS source temperatures were 250°C. The modulation time was 2 s (0.8 s for hot pulse time and 0.2 s for cold pulse time); the modulator temperature was kept at 20 ºC offset (above secondary oven). The ToFMS was operated at a spectrum storage rate of 100 spectra/s. The mass spectrometer was operated in the EI mode at 70 eV using a range of *m/z* 35-350 and the detector voltage was -1561 V. Total ion chromatograms were processed using the automated data processing software ChromaTOF® (LECO) at a signal-to-noise threshold of 100. Contour plots were used to evaluate the overall separation quality and for manual peak identification. The mass spectrum and retention times ($^{1}t_R$ and $^{2}t_R$ - from the first and second dimensions, respectively) of each analyte were collected. Linear retention index (LRI) values were also determined (**Table 1**) using a C_8-C_{20} *n*-alkane series (the solvent *n*-hexane was used as C_6 standard) and calculated according to the van Den Dool and Kratz equation [36]. The Deconvoluted Total Ion Current GC×GC area data were used as an approach to estimate the relative content of each analyte or to calculate its concentration.

2.4. Statistical analysis

Peak areas of polar VOCs were extracted from the chromatograms and used to build the data matrices which consisted of 3 observations per fiber and/or fiber/condition (time and temperature of desorption) and 19 variables (analytes). Two heatmaps were constructed using: i) the data from the commercial SPME fibers in two desorption conditions, and ii) the data from the commercial SPME fibers and the zwitterionic PIL in the optimal desorption condition. Each

variable area was auto scaled prior to the hierarchical cluster analysis (HCA) using MetaboAnalyst 3.0 (web software, The Metabolomics Innovation Centre (TMIC), Canada) [37]. HCA is an exploratory tool, applied to characterize the data set, revealing natural groupings (or clusters) within it, through the representation of a dendrogram (tree diagram) and a heatmap. Squared Euclidean distances were used, and the clustering algorithm used was Ward's minimum variance.

One-way analysis of variance (ANOVA) followed by a multiple comparison test (Tukey's HSD) using the GraphPad Prism® version 6 for Windows (30-day trial version, GraphPad Software, San Diego California, USA), was applied to evaluate the effect of desorption conditions (time and temperature). Differences corresponding to $p < 0.05$ were considered significant.

3. Results and Discussion

3.1. Implementation of Chromatographic Conditions

Before the implementation of the GC×GC-ToFMS instrumental conditions, the SPME extraction parameters were established, based on the criteria explained below. Extractions were performed at 30 °C for 20 min from the headspace containing 50 μL of the working solution with the 19 analytes using a DVB/CAR/PDMS fiber, followed by the thermal desorption in the GC×GC port.

Regarding the extraction conditions, the DVB/CAR/PDMS sorbent coating was selected as a starting point as it is recommended for the extraction of a wide range of analytes, including polar ones. The DVB/CAR/PDMS sorbent coating is produced using three different polymers which gives it a synergistic effect between adsorption and absorption. This mutually synergetic effect promotes a higher retention capacity and, consequently, a higher sensitivity [38,39]. For these reasons and to assure all the 19 standards would be detected, the chromatographic conditions were implemented using the DVB/CAR/PDMS coating.

In order to mimic a condition in the present study that may represent the capture of the analytes released from human remains (or even from soil or other locations associated with body decomposition) at room temperature, a volume of 50 μL of the working solution containing all of the 19 analytes was introduced into a 25 mL vial and thermostated at *ca*. 30°C. This condition may promote volatilization of the analytes and, during the extraction, enable mass transfer of analytes from the headspace to the coating. As overall mass transfer to the fiber is typically limited by mass transfer rates from the solid and/or liquid sample to the headspace

[40], this volatilization may simulate the real conditions of collection of death-related VOCs stated in the literature [9,15,18–20].

SPME, as a measure of free concentration of analytes in the sample, is an equilibrium extraction technique. Therefore, selection of the optimum extraction time is one of the critical steps in SPME method development. Extraction time selection is always a compromise between the length, sensitivity and reproducibility of the method. Equilibrium extraction provides the highest sensitivity and reproducibility, but in most SPME-GC applications, pre-equilibrium conditions are used since equilibrium extraction times tend to be longer, and thus impractical. Both equilibrium and pre-equilibrium extractions need precise and perfectly repeatable timing, although for the latter condition, timing is more critical [40,41]. The chosen extraction time was 20 min, which corresponds to a pre-equilibrium situation, since it represents a good compromise between practicality and good analytical performance [28].

As a preliminary study, different sets of GC columns and chromatographic conditions were screened (data not shown) in order to obtain the appropriate chromatographic resolution and sensitivity for all the 19 analytes. For instance, conventional and reversed phase column combinations for GC×GC-ToFMS were evaluated concerning their suitability for the analysis of the set of 19 polar analytes. From a practical point of view, a conventional column set (nonpolar ^{1}D × polar ^{2}D) was tested, as it is the most common column set used in the laboratory for the analysis of a wide range of samples. However, an inappropriate separation of the analytes with large peak width was observed, especially for the most polar compounds as the organic acids (**Fig. 1S**). Thus, a reversed GC×GC column set Carbowax/BTR and Equity 5 (polar ^{1}D × nonpolar ^{2}D), both with 0.25 mm I.D., 0.25 µm film thickness, was examined and provided a better separation of the analytes with smaller peak width (**Fig. 2** and **Fig. 1S**). Previous studies also confirmed that the use of a column set with the same diameters in primary and secondary columns yields a near-theoretical maximum in peak capacity gain, i.e. increases the number of components that the system can resolve (quantifiably and identifiably separate) [42]. The results indicated that reversed phase column set presented advantages compared to a conventional column set regarding the analytes separation, and also allowd to infer that higher sensitivity and accuracy for the quantification will be improved due to smaller peak width of the compounds [43].

Insert Fig. 2

After extraction by HS-SPME and analysis by GC×GC-ToFMS under the implemented conditions (*sections 2.2 and 2.3*), a peak apex (**Fig. 2**) was constructed based on the retention times on the first and the second dimensions, representing a schematic illustration of the peak distribution map for the working solution run under stated conditions. This figure reveals that the instrumental parameters previously defined promoted the appropriate chromatographic resolution and that the 19 analytes tend to be organized by chemical families and are distributed through the first dimension especially according to their volatility and carbon number. The retention times of each analyte on the ^{1}D and ^{2}D column and the linear retentions indexes are listed in **Table 1**.

Desorption time and temperature conditions are very important to guarantee quantitative desorption of the analytes from the fibers and avoid *carry over.* Since zwitterionic PILs possess a maximum operating temperature of 175 °C [31], two desorption conditions were tested on the commercial fibers to assess the impact of a lower desorption temperature on the chromatographic signal. Therefore, the commercial SPME fibers were tested under their usual operating desorption temperature (250 °C) [44–46] and under the zwitterionic PILs optimal temperature (175 °C). Due to the high volatility of the compounds under study, the desorption times were relatively low. Compared to the desorption at 250 °C for 60 s, the desorption conditions at 175 °C for 180 s promoted a significant increase in chromatographic areas of the analytes from 39 to 152% for DVB/CAR/PDMS (**Fig. 3** and **Table 1S**). Using the PA and the PDMS/DVB fibers, increments from 3 to 83% and from 5 to 188%, respectively, were observed only for the components that in general exhibit the higher vapor pressure and lower boiling point (**Table 1)** (compounds with peak number 1 to 7). The PDMS/DVB fiber exhibited lower chromatographic areas at both desorption conditions, while DVB/CAR/PDMS and PA showed the highest chromatographic areas for the desorption conditions of 175 °C for 180 s (**Fig. 3** and **Fig. 2S**).

Insert Fig. 3

The temperature and desorption time selected to compare the performance of the commercial coatings with the zwitterionic PIL were 175 °C for 180 s, respectively.

3.2. Evaluation of Coatings' Extraction Efficiency

A hierarchical cluster analysis combined with the heatmap representation was constructed to evaluate the SPME coatings´ extraction efficiency. The heatmap (**Fig. 4**) shows a graphical representation of the chromatographic data achieved for the 19 standards, allowing a rapid visual evaluation of the fibers' extraction efficiency. The chromatic scale of the heatmap shows the relative amount of each standard (from dark blue, minimum, to dark red, maximum).

Insert Fig. 4

It is possible to observe the formation of two main clusters (**Fig. 4**): one cluster contains the fibers with the highest extraction efficiency (DVB/CAR/PDMS followed by PA), and the other cluster contains the fibers with the lower extraction efficiency (PIL and PDMS/DVB), with the PDMS/DVB the fiber exhibiting the lowest efficiency. The behaviour of the different fibers may be explained based on their specific characteristics, as reported in **Table 2**. The type of the phase determines the polarity of the coating, which can provide selectivity by enhancing the affinity of the coating for polar analytes compared with nonpolar fiber coatings. Also, the mechanism of extraction is determined by whether a coating is an absorbent type, or an adsorbent type and the thickness of the coating determines the analyte capacity of the fiber [39].

Insert Table 2

As the DVB/CAR/PDMS and PDMS/DVB fibers extract via an adsorptive-type mechanism, the analytes interact primarily with the surface of the sorbent coating instead of partitioning into the entire coating and, therefore, the sensitivity of these fibers depend on other factors such as the surface area and porosity of the material, among others [39,47]. The lower extraction efficiency of the PDMS/DVB fiber may be due to the porosity properties of the DVB, that represent some concerns about the analytes displacement and has difficulty to extract analytes with low molecular weight, as the case of the 19 analytes under study with molecular weight ranging between 73.10 for *N*,*N*-dimethylformamide to 157.26 g mol^{-1} to *N*,*N*-dibutylformamide. The DVB/CAR/PDMS fiber, which combines three materials, was developed to overcome the limitations of the CAR/PDMS in the desorption of higher molecular weight analytes and PDMS/DVB in difficulty of extracting analytes with low molecular weights. The DVB/CAR/PDMS coating contains both adsorbents that are layered to extend the molecular weight range of analytes extracted with one SPME fiber and the combination with

the PDMS confer the its bipolar character [39], which explain the best performance of this fiber (**Fig. 4** and **Fig. 3S**).

In fibers with absorptive-type mechanism such as PA [39] and the zwitterionic PIL [31], diffusion of the analytes through the sorbent coating is a dominant effect. Therefore, analytes can freely partition into the sorbent, with little competition among analytes, and the concentration of each analyte at equilibrium is less affected by the presence of other analytes. Thus, the polar PA fiber with an 85 µm of thickness exhibited sensitivity for all the analytes (**Fig. 4** and **Fig. 3S**). This may be also attributed to the polar character of the analytes as expressed by their Log P values that ranged from -1.0 for *N,N*-dimethylformamide to 2.8 for 3-octanol. The lower extractive efficiency of PIL compared to PA may be due to its lower film thickness (18 µm ± 6), *ca*. 4 times smaller than that of PA. On-going work is devoted to improving the coating process to obtain thicker sorbent coatings to increase the sensitivity of the method.

In addition to fiber extraction efficiency, it was also investigated as to whether the data obtained is representative of headspace composition, (i.e., the relative concentration of each analyte in the vial – 3750 ng/vial for alcohols and formamides, 2500 ng/vial for acids and 1250 ng/vial for all the other standards). When comparing the representativeness of the headspace composition of the different coatings, it is noticeable that the DVB/CAR/PDMS fiber doesn't achieve that goal as well as the others (**Fig. 4**). The hierarchical clustered heatmap also unveils that in a secondary dendrogram (in vertical position) the analytes are organized according to their concentration, except for the data observed with the DVB/CAR/PDMS fiber. This fiber seems to exhibit higher sensitivity for the analytes present at lower concentration (1250 ng/vial), as they present higher chromatographic areas. Except for 2-acetylfuran and benzaldehyde, the analytes captured with higher efficiency by the DVB/CAR/PDMS fiber are, in general, those with high volatility, which allows to infer a competition effect. In fact, previous studies [31,48] also reported that absorption is the primary extraction mechanism of the zwitterionic PIL, a behaviour similar to the commercially-available PA, and different than that observed for adsorbent type fiber such as DVB/CAR/PDMS and PDMS/DVB, for which a competitive extraction mechanism is typical. Thus, although the DVB/CAR/PDMS fiber has the best extraction efficiency, it doesn't possess all the properties needed for this application. Both PA and the zwitterionic PIL volatile profiles are representative of the headspace composition (**Fig. 4**) with PA exhibiting better extraction efficiency than the zwitterionic PIL.

Since PA and zwitterionic PIL exhibited the best performance to study these polar analytes in the headspace mode, they were selected to evaluate the analytical performance of the HS-

SPME/ GC×GC-ToFMS methodology through the construction of calibration curves with six concentrations and calculation of the respective analytical figures of merit.

3.3. Analytical Performance of the Method

Matrix-matched calibrations in diluted ethanolic solution with 19 analytes were developed for the PA and PIL fibers. The primary working solution possessed the following concentrations of analytes: 3750 ng/vial for alcohols and formamides, 2500 ng/vial for acids and 1250 ng/vial for all the other standards. This solution was then diluted 5, 10, 15, 20 and 25 times to make calibration curves. **Table 3** lists analytical figures of merit of the curves.

Insert Table 3

The calibrations presented wide linear ranges for both fibers, ranging from 150 to 3750 ng for alcohols and formamides, from 100 to 2500 ng for acids and from 50 to 1250 ng for the other standards.

The sensitivity of the method was evaluated using calibration slopes (**Table 3**) that ranged from 0.258×10^{-4} to 10.0×10^{-4} for PA and from 0.215×10^{-4} to 7.26×10^{-4} for the zwitterionic PIL. The slope with the lowest value belongs to hexanoic acid and the one with the highest value belongs to 2,4-pentanedione for both fibers. Slightly higher sensitivities were achieved for all analytes using PA.

The limits of detection (LOD) were estimated as the concentration corresponding to three times the signal-to-noise ratio (**Table 3**). The obtained values ranged between 2.1 ng (butanoic acid ethyl ester) and 283.8 ng (hexanoic acid) for PA and between 2.4 ng (butanoic acid ethyl ester) and 301.9 ng (benzaldehyde) for the zwitterionic PIL. Except benzaldehyde, in general, the LODs obtained with the zwitterionic PIL were slightly lower than the ones obtained with PA.

The reproducibility of the method, expressed as RSD, was evaluated at a spiked level of 3750 ng/vial for alcohols and formamides, 2500 ng/vial for acids and 1250 ng/vial for the other standards. The RSD values ranged from 0.50 (1-pentanol) to 18 % (pentanoic acid) for PA, except for hexanoic acid that had an RSD of 44 %, and from 2.9 (phenylethyl alcohol) to 17 % (butanoic acid ethyl ester) for the zwitterionic PIL. The relative recovery (RR) was calculated at the same spiked level as the ratio of the predicted concentration obtained using matrix-matched calibrations of **Table 3** and the spiked concentration and its values ranged from 99.1

to 102 % for PA and from 100 to 103 % for the zwitterionic PIL, except for benzaldehyde that had a RR of 93.7 %. The RR values were acceptable for both fibers.

4. Conclusions

A methodology based on HS-SPME/GC×GC-ToFMS was shown to be suitable for the determination of 19 polar analytes associated with the unique odour created by decomposing bodies, in conditions that mimic the capture of the analytes released from human remains (or even from soil or other locations associated with body decomposition). Firstly, the GC×GC-ToFMS experimental parameters were implemented, and the reversed phase column set (polar ^{1}D × nonpolar ^{2}D), with the same diameters in primary and secondary columns (0.25 mm I.D., 0.25 µm film thickness), presented advantages compared to the conventional column set (nonpolar ^{1}D × polar ^{2}D) regarding the analytes separation. A subsequent hierarchical cluster analysis combined with the heatmap representation was shown to be an appropriate approach to evaluate similarities and differences between the four coatings, and revealed that they were all able to capture the 19 analytes from the headspace, however they exhibited distinct differences in performance. The sorbent coatings can be positioned in the following ascending order of extraction efficiency: PDMS/DVB < PIL < PA < DVB/CAR/PDMS. The lower extraction efficiency of the PDMS/DVB fiber may be due to the porous properties of the DVB and the consequent difficulty of extracting analytes with low molecular weight, as the case of the 19 analytes under study. On the other hand, DVB/CAR/PDMS, which combines three sorbents, exhibited the highest extraction efficiency, but the volatile profile obtained is not representative of the headspace composition. This behavior may be attributed to higher sensitivity for the analytes with high volatility, which infers a competition effect. PA and zwitterionic PIL fibers, both with absorptive-type mechanism, provided a good balance between representativeness of headspace composition and extraction efficiency. For this reason, they were selected to evaluate the analytical performance of the HS-SPME/ GC×GC-ToFMS methodology. The calibrations provided wide linear ranges for both fibers, ranging from 150 to 3750 ng for alcohols and formamides, from 100 to 2500 ng for acids and from 50 to 1250 ng for the other standards. The reproducibility (with relative standard deviation lower than 18 %, depending on the analyte) and relative recoveries (higher than 99.1 %, depending on the analyte) were similar and acceptable for both fibers.

In summary, PA and PIL may represent useful tools to respond to current challenges in forensic taphonomy, as these sorbent coatings, combined with GC×GC-ToFMS analysis,

allowed the determination of the 19 polar analytes under study at ng level, providing a profile representative of the headspace composition. The zwitterionic PIL, with *ca*. 4 times smaller film thickness than PA, still has potential to provide the best performance and work is currently in progress to obtain thicker sorbent coatings. This study performed using standards and conditions that mimic the odor of body decomposition represents the first and mandatory step in the construction of a methodology. Future work is planned for the analysis of real samples, such as animal and human remains and the soil in which they decompose.

Furthermore, the combination of GC×GC-ToFMS with SPME may represent a useful tool for a streamlined evaluation of post-mortem changes of human remains by constructing a multiple attribute methodology (MAM) workflow taking advantages of their sensitivity and high throughput attributes. The current challenge in criminal and judicial areas are based on increasing pressure from private and public institutions and the push to increase speed on the response, improving the accuracy and robustness on the results. This approach is also in line with the analytical green chemistry guidelines, as solvents or toxic reagents are avoided, where direct extraction of analytes in a multi-analyte methodology is performed. Furthermore, the approach has potential to be extended to more polar analytes, such as excretion metabolites in the context of forensic toxicology, either for drugs of abuse or poisonings.

Acknowledgements Thanks are due to FCT/MEC for the financial support to QOPNA (UID/QUI/00062/2019) and LAQV-REQUIMTE (UIDB/50006/2020) Research Units, through national funds and where applicable co-financed by the FEDER, within the PT2020 Partnership Agreement. JLA acknowledges the Chemical Measurement and Imaging Program at the National Science Foundation (CHE-1709372).

Declaration of competing interest

The authors declare that they have no known competing financial interests or personal relationships that could have appeared to influence the work reported in this paper..

Appendix A. Supplementary data

Supplementary data to this article can be found online at https://doi.org/xx.xxxx/j.microc.2020.xxxxxx.

References

[1] J. Pokines, S.A. Symes, Manual of Forensic Taphonomy, 1st ed., CRC Press, 2013.

[2] A.E. Rattenbury, Forensic Ecogenomics, 1st ed., Academic Press, 2018.

[3] K. Ritz, L. Dawson, D. Miller, Criminal and environmental soil forensics, Crim. Environ. Soil Forensics. (2009) 1–519. https://doi.org/10.1007/978-1-4020-9204-6.

[4] M.A. Iqbal, M. Ueland, S.L. Forbes, Recent advances in the estimation of post-mortem interval in forensic taphonomy, Aust. J. Forensic Sci. 0618 (2018) 1–17. http://doi.org/10.1080/00450618.2018.1459840.

[5] C.J. Rogers, Dating death: Forensic taphonomy and the postmortem interval thesis submitted for the Degree of doctor of philosophy, (2010) 249.

[6] M. Mora-Ortiz, M. Trichard, A. Oregioni, S.P. Claus, Thanatometabolomics: introducing NMR-based metabolomics to identify metabolic biomarkers of the time of death, Metabolomics. 15 (2019) 1–11. https://doi.org/10.1007/s11306-019-1498-1.

[7] S. Paczkowski, S. Schütz, Post-mortem volatiles of vertebrate tissue, Appl. Microbiol. Biotechnol. 91 (2011) 917–935. https://doi.org/10.1007/s00253-011-3417-x.

[8] S.L. Forbes, K.A. Perrault, Decomposition Odour Profiling in the Air and Soil Surrounding Vertebrate Carrion, PLoS One. 9 (2014) e95107. https://doi.org/10.1371/journal.pone.0095107.

[9] E. Rosier, S. Loix, W. Develter, W. Van De Voorde, J. Tytgat, E. Cuypers, The search for a volatile human specific marker in the decomposition process, PLoS One. 10 (2015) 1–15. https://doi.org/10.1371/journal.pone.0137341.

[10] B.B. Dent, S.L. Forbes, B.H. Stuart, Review of human decomposition processes in soil, Environ. Geol. 45 (2004) 576–585. https://doi.org/10.1007/s00254-003-0913-z.

[11] B. Kalinová, H. Podskalská, J. Růžička, M. Hoskovec, Irresistible bouquet of death-how are burying beetles (Coleoptera: Silphidae: Nicrophorus) attracted by carcasses, Naturwissenschaften. 96 (2009) 889–899. https://doi.org/10.1007/s00114-009-0545-6.

[12] S. Stadler, P.H. Stefanuto, M. Brokl, S.L. Forbes, J.F. Focant, Characterization of volatile organic compounds from human analogue decomposition using thermal desorption coupled to comprehensive two-dimensional gas chromatography-time-of-flight mass spectrometry, Anal. Chem. 85 (2013) 998–1005. https://doi.org/10.1021/ac302614y.

[13] M. Statheropoulos, A. Agapiou, C. Spiliopoulou, G.C. Pallis, E. Sianos, Environmental aspects of VOCs evolved in the early stages of human decomposition, Sci. Total Environ.

385 (2007) 221–227. https://doi.org/10.1016/j.scitotenv.2007.07.003.

[14] F. Verheggen, K.A. Perrault, R.C. Megido, L.M. Dubois, F. Francis, E. Haubruge, S.L. Forbes, J.F. Focant, P.H. Stefanuto, The Odor of Death: An Overview of Current Knowledge on Characterization and Applications, Bioscience. 67 (2017) 600–613. https://doi.org/10.1093/biosci/bix046.

[15] P. Armstrong, K.D. Nizio, K.A. Perrault, S.L. Forbes, Establishing the volatile profile of pig carcasses as analogues for human decomposition during the early postmortem period, Heliyon. 2 (2016) 1–24. https://doi.org/10.1016/j.heliyon.2016.e00070.

[16] A.A. Vass, Odor mortis, Forensic Sci. Int. 222 (2012) 234–241. https://doi.org/10.1016/j.forsciint.2012.06.006.

[17] B. Gruber, B.A. Weggler, R. Jaramillo, K.A. Murrell, P.K. Piotrowski, F.L. Dorman, Comprehensive two-dimensional gas chromatography in forensic science: A critical review of recent trends, TrAC - Trends Anal. Chem. 105 (2018) 292–301. https://doi.org/10.1016/j.trac.2018.05.017.

[18] M. Statheropoulos, A. Agapiou, E. Zorba, K. Mikedi, S. Karma, G.C. Pallis, C. Eliopoulos, C. Spiliopoulou, Combined chemical and optical methods for monitoring the early decay stages of surrogate human models, Forensic Sci. Int. 210 (2011) 154–163. https://doi.org/10.1016/j.forsciint.2011.02.023.

[19] J. Dekeirsschieter, F.J. Verheggen, M. Gohy, F. Hubrecht, L. Bourguignon, G. Lognay, E. Haubruge, Cadaveric volatile organic compounds released by decaying pig carcasses (Sus domesticus L.) in different biotopes, Forensic Sci. Int. 189 (2009) 46–53. https://doi.org/10.1016/j.forsciint.2009.03.034.

[20] S.L. Forbes, A.N. Troobnikoff, M. Ueland, K.D. Nizio, K.A. Perrault, Profiling the decomposition odour at the grave surface before and after probing, Forensic Sci. Int. 259 (2016) 193–199. https://doi.org/10.1016/j.forsciint.2015.12.038.

[21] S. Petronilho, M.A. Coimbra, S.M. Rocha, A critical review on extraction techniques and gas chromatography based determination of grapevine derived sesquiterpenes, Anal. Chim. Acta. 846 (2014) 8–35. https://doi.org/10.1016/j.aca.2014.05.049.

[22] J.M.F. Nogueira, Novel sorption-based methodologies for static microextraction analysis: A review on SBSE and related techniques, Anal. Chim. Acta. 757 (2012) 1–10. https://doi.org/10.1016/j.aca.2012.10.033.

[23] J.R.B. de Souza, F.F.G. Dias, J.D. Caliman, F. Augusto, L.W. Hantao, Opportunities for green microextractions in comprehensive two-dimensional gas chromatography / mass spectrometry-based metabolomics – A review, Anal. Chim. Acta. 1040 (2018) 1–18.

https://doi.org/10.1016/j.aca.2018.08.034.

[24] A. Spietelun, Ł. Marcinkowski, M. de la Guardia, J. Namieśnik, Recent developments and future trends in solid phase microextraction techniques towards green analytical chemistry, J. Chromatogr. A. 1321 (2013) 1–13. https://doi.org/10.1016/j.chroma.2013.10.030.

[25] N. Reyes-Garcés, E. Gionfriddo, G.A. Gómez-Ríos, M.N. Alam, E. Boyacl, B. Bojko, V. Singh, J. Grandy, J. Pawliszyn, Advances in Solid Phase Microextraction and Perspective on Future Directions, Anal. Chem. 90 (2018) 302–360. https://doi.org/10.1021/acs.analchem.7b04502.

[26] M.E. Cablk, E.E. Szelagowski, J.C. Sagebiel, Characterization of the volatile organic compounds present in the headspace of decomposing animal remains, and compared with human remains, Forensic Sci. Int. 220 (2012) 118–125. https://doi.org/10.1016/j.forsciint.2012.02.007.

[27] K. Perrault, B. Stuart, S. Forbes, A Longitudinal Study of Decomposition Odour in Soil Using Sorbent Tubes and Solid Phase Microextraction, Chromatography. 1 (2014) 120–140. https://doi.org/10.3390/chromatography1030120.

[28] E.M. Hoffman, A.M. Curran, N. Dulgerian, R.A. Stockham, B.A. Eckenrode, Characterization of the volatile organic compounds present in the headspace of decomposing human remains, Forensic Sci. Int. 186 (2009) 6–13. https://doi.org/10.1016/j.forsciint.2008.12.022.

[29] L.E. Degreeff, K.G. Furton, Collection and identification of human remains volatiles by non-contact, dynamic airflow sampling and SPME-GC/MS using various sorbent materials, Anal. Bioanal. Chem. 401 (2011) 1295–1307. https://doi.org/10.1007/s00216-011-5167-0.

[30] M.J. Trujillo-Rodríguez, H. Nan, M. Varona, M.N. Emaus, I.D. Souza, J.L. Anderson, Advances of Ionic Liquids in Analytical Chemistry, Anal. Chem. 91 (2019) 505–531. https://doi.org/10.1021/acs.analchem.8b04710.

[31] I. Pacheco-Fernández, M.J. Trujillo-Rodríguez, K. Kuroda, A.L. Holen, M.B. Jensen, J.L. Anderson, Zwitterionic polymeric ionic liquid-based sorbent coatings in solid phase microextraction for the determination of short chain free fatty acids, Talanta. 200 (2019) 415–423. https://doi.org/10.1016/j.talanta.2019.03.073.

[32] A.C. Cole, J.L. Jensen, I. Ntai, K.L.T. Tran, K.J. Weaver, D.C. Forbes, J.H. Davis, Novel brønsted acidic ionic liquids and their use as dual solvent-catalysts, J. Am. Chem. Soc. 124 (2002) 5962–5963. https://doi.org/10.1021/ja026290w.

[33] H. Satria, K. Kuroda, T. Endo, K. Takada, K. Ninomiya, K. Takahashi, Efficient Hydrolysis of Polysaccharides in Bagasse by in Situ Synthesis of an Acidic Ionic Liquid after Pretreatment, ACS Sustain. Chem. Eng. 5 (2017) 708–713. https://doi.org/10.1021/acssuschemeng.6b02055.

[34] Q.Q. Baltazar, J. Chandawalla, K. Sawyer, J.L. Anderson, Interfacial and micellar properties of imidazolium-based monocationic and dicationic ionic liquids, Colloids Surfaces A Physicochem. Eng. Asp. 302 (2007) 150–156. https://doi.org/10.1016/j.colsurfa.2007.02.012.

[35] T.D. Ho, B.R. Toledo, L.W. Hantao, J.L. Anderson, Chemical immobilization of crosslinked polymeric ionic liquids on nitinol wires produces highly robust sorbent coatings for solid-phase microextraction, Anal. Chim. Acta. 843 (2014) 18–26. https://doi.org/10.1016/j.aca.2014.07.034.

[36] H. van Den Dool, P.D. Kratz, A generalization of the retention index system including linear temperature programmed gas—liquid partition chromatography, J. Chromatogr. 11 (1963) 463–471.

[37] J. Xia, I. V. Sinelnikov, B. Han, D.S. Wishart, MetaboAnalyst 3.0-making metabolomics more meaningful, Nucleic Acids Res. 43 (2015) W251–W257. https://doi.org/10.1093/nar/gkv380.

[38] H. Piri-Moghadam, M.N. Alam, J. Pawliszyn, Review of geometries and coating materials in solid phase microextraction: Opportunities, limitations, and future perspectives, Anal. Chim. Acta. 984 (2017) 42–65. https://doi.org/10.1016/j.aca.2017.05.035.

[39] S.R. E., SPME Commercial Devices and Fibre Coatings, in: J. Pawliszyn (Ed.), Handb. Solid Phase Microextraction, Chemical Industry Press, 2009: pp. 86–115.

[40] J. Pawliszyn, Theory of Solid Phase Microextraction, in: J. Pawliszyn (Ed.), Handb. Solid Phase Microextraction, Chemical Industry Press, 2009: pp. 13–54.

[41] L. Kudlejova, S. Risticevic, D. Vuckovic, Solid-Phase Microextraction Method Development, in: J. Pawliszyn (Ed.), Handb. Solid Phase Microextraction, Chemical Industry Press, 2009: pp. 173–214.

[42] M.S. Klee, J. Cochran, M. Merrick, L.M. Blumberg, Evaluation of conditions of comprehensive two-dimensional gas chromatography that yield a near-theoretical maximum in peak capacity gain, J. Chromatogr. A. 1383 (2015) 151–159. https://doi.org/10.1016/j.chroma.2015.01.031.

[43] M. Jennerwein, M. Eschner, T. Wilharm, T. Gröger, R. Zimmermann, Evaluation of

reversed phase versus normal phase column combination for the quantitative analysis of common commercial available middle distillates using GC × GC-TOFMS and Visual Basic Script, Fuel. 235 (2019) 336–338. https://doi.org/10.1016/j.fuel.2018.07.081.

[44] C. Martins, T. Brandão, A. Almeida, S.M. Rocha, Unveiling the lager beer volatile terpenic compounds, Food Res. Int. 114 (2018) 199–207. https://doi.org/10.1016/j.foodres.2018.07.048.

[45] D. Silva, E. Arend, S.M. Rocha, A. Rudnitskaya, L. Delgado, A. Moreira, J. Carvalho, The impact of exercise training on the lipid peroxidation metabolomic profile and respiratory infection risk in older adults, Eur. J. Sport Sci. 19 (2019) 384–393. https://doi.org/10.1080/17461391.2018.1499809.

[46] I. Baptista, M. Santos, A. Rudnitskaya, J.A. Saraiva, A. Almeida, S.M. Rocha, A comprehensive look into the volatile exometabolome of enteroxic and non-enterotoxic Staphylococcus aureus strains, Int. J. Biochem. Cell Biol. 108 (2019) 40–50. https://doi.org/10.1016/j.biocel.2019.01.007.

[47] N.H. Godage, E. Gionfriddo, A critical outlook on recent developments and applications of matrix compatible coatings for solid phase microextraction, TrAC - Trends Anal. Chem. 111 (2019) 220–228. https://doi.org/10.1016/j.trac.2018.12.019.

[48] T.D. Ho, W.T.S. Cole, F. Augusto, J.L. Anderson, Insight into the extraction mechanism of polymeric ionic liquid sorbent coatings in solid-phase microextraction, J. Chromatogr. A. 1298 (2013) 146–151. https://doi.org/10.1016/j.chroma.2013.05.009.

Figure Captions

Fig. 1. Illustration of the chemical structures of the (A) zwitterionic ionic liquid (ZIL) monomer and the (B) ionic liquid (IL) crosslinker.

Fig. 2. Peak apex representing 2D chromatographic space of the analytes under study. Peak assignment is shown in Table 1.

Fig. 3. Peak areas obtained from the implemented HS-SPME/GC×GC-TOFMS methodology to evaluate two desorption conditions (175 ˚C for 180 s and 250 ˚C for 60 s) for the three commercial coatings (DVB/CAR/PDMS, PDMS/DVB and PA), using a work solution with the following concentrations: 3750 ng/vial for alcohols and formamides, 2500 ng/vial for acids and 1250 ng/vial for all the other standards. The PDMS/DVB fiber at both desorption conditions exhibited the lower chromatographic areas, while DVB/CAR/PDMS and PA showed the highest chromatographic areas for the desorption condition at 175 °C for 180 s.

Fig. 4. Heatmap constructed using the peak areas obtained from the implemented HS-SPME/GC×GC-TOFMS methodology to evaluate the extraction efficiency of DVB/CAR/PDMS, PDMS/DVB, PA and PIL fibers. A work solution with the following concentrations was used: 3750 ng/vial for alcohols and formamides, 2500 ng/vial for acids and 1250 ng/vial for all the other standards. The content of each compound was illustrated through a chromatic scale (from dark blue, minimum, to dark red, maximum). Dendrogram for the HCA results using Ward's cluster algorithm to the data set was also included. Two main clusters are observed: one clusters contains the fibers with the highest extraction efficiency (DVB/CAR/PDMS followed by PA), and the other cluster contains the fibers with the lower extraction efficiency (PIL and PDMS/DVB), being the PDMS/DVB the fiber that exhibited the lowest efficiency.

717

Table 1

Chromatographic and molecular data of the analytes under study.

Peak Number	Compound Name	[1]RT (s)[a]	[2]RT (s)[b]	LRI[c]	Chemical Structure	Chemical Family	Molecular Formula	Log P[d]	VP (mm Hg)[e]	BP (°C)[f]
1	Butanoic acid, ethyl ester	228	0.750	978	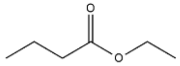	Ester	$C_6H_{12}O_2$	1.3	12.80 (25˚C)	120
2	Dimethyl disulfide	260	0.590	999	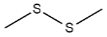	Sulfur-containing	$C_2H_6S_2$	1.8	28.73 (25˚C)	110
3	2,4-Pentanedione	400	0.540	1108	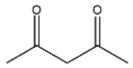	Ketone	$C_5H_8O_2$	0.4	2.96 (20˚C)	138
4	3-Methyl-1-butanol	418	0.490	1119	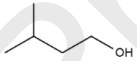	Alcohol	$C_5H_{12}O$	1.2	2.37 (25˚C)	131
5	2,3-Heptanedione	438	0.680	1136	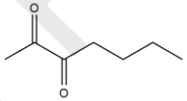	Ketone	$C_7H_{12}O_2$	1.0	3.98 (25˚C)	64
6	3-Octanone	468	0.950	1159	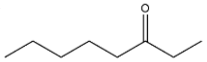	Ketone	$C_8H_{16}O$	2.3	1.50 (25˚C)	170
7	1-Pentanol	472	0.500	1160	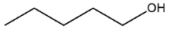	Alcohol	$C_5H_{12}O$	1.6	1.67 (25˚C)	139
8	2,6-Dimethylpyrazine	562	0.620	1232	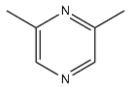	Nitrogen-containing	$C_6H_8N_2$	0.5	0.31 (25˚C)	154
9	*N,N*-Dimethylformamide	572	0.470	1236	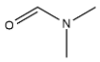	Nitrogen-containing	C_3H_7NO	-1.0	3.87 (25˚C)	153

10	1-Hexanol	604	0.530	1263	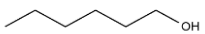	Alcohol	$C_6H_{14}O$	2.0	0.93 (25˚C)	158
11	3-Octanol	654	0.680	1302	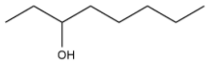	Alcohol	$C_8H_{18}O$	2.8	0.51 (25˚C)	175
12	2-Hexen-1-ol	672	0.490	1317	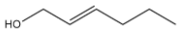	Alcohol	$C_6H_{12}O$	1.4	0.87 (25˚C)	158
13	2-Acetylfuran	794	0.480	1415	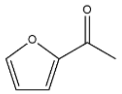	Furan	$C_6H_6O_2$	0.5	0.77 (25˚C)	183
14	Benzaldehyde	810	0.520	1429	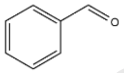	Aldehyde (aromatic)	C_7H_6O	1.5	1.27 (25˚C)	179
15	Pentanoic acid	1086	0.400	1671	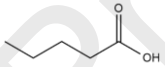	Carboxylic acid	$C_5H_{10}O_2$	1.4	0.45 (25˚C)	185
16	*N*,*N*-Dibutylformamide	1094	0.750	1677	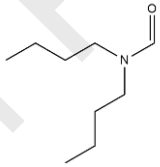	Nitrogen-containing	$C_9H_{19}NO$	2.2	<1 (20˚C)	120
17	Hexanoic acid	1202	0.420	1777	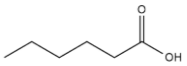	Carboxylic acid	$C_6H_{12}O_2$	1.9	1.6 (25˚C)	205
18	Benzyl alcohol	1222	0.440	1793	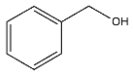	Alcohol (aromatic)	C_7H_8O	1.1	0.09 (25˚C)	205

19	Phenylethyl alcohol	1264	0.490	1831	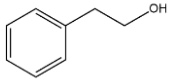	Alcohol (aromatic)	$C_8H_{10}O$	1.4	0.09 (25˚C)	218

[a] Retention time for first dimension
[b] Retention time for second dimension
[c] Linear Retention Index obtained experimentally through the modulated chromatogram
[d] Data obtained from PubChem Database
[e] Vapor pressure, data obtained from The Good Scents Company Information System
[f] Boiling Point, data obtained from ChemSpider Database

Table 2

Characteristics of the four studied SPME sorbent coatings.

Type of coating	Core type	Extraction mechanism	Polarity	Coating Thickness (µm)
PA	Fused silica	Absorption	Polar	85
PDMS/DVB	Stableflex	Adsorption	Bipolar	65
DVB/CAR/PDMS	Stableflex	Adsorption	Bipolar	50/30
Zwitterionic PIL	Nitinol	Absorption	Polar	18 ± 6

Table 3
Analytical figures of merit of the HS-SPME/GC×GC-ToFMS methodology after performing matrix-matched calibration of 19 chemical standards.

Analytes	Working Range (ng/vial)	Slope ($\cdot 10^{-4}$)		LOD[a] (ng)		%RR[b] (%RSD[c])	
		PA	PIL	PA	PIL	PA	PIL
Butanoic acid ethyl ester	50 - 1250	9.69	4.96	2.1	2.4	101 (3.4)	101 (17)
Dimethyl disulfide	50 - 1250	9.97	5.08	13.0	4.2	101 (3.6)	100 (6.7)
2,4-Pentanedione	50 - 1250	10.0	7.26	36.7	29.1	101 (13)	100 (5.1)
3-Methyl-1-butanol	150 - 3750	3.33	2.23	61.5	52.3	101 (8.5)	100 (1.6)
2,3-Heptanedione	50 - 1250	2.45	0.723	4.7	5.0	99.1 (8.3)	101 (11)
3-Octanone	50 - 1250	7.06	2.53	9.1	6.6	102 (3.6)	101 (10)
1-Pentanol	150 - 3750	3.35	2.14	56.9	40.5	102 (0.50)	103 (3.1)
2,6-Dimethylpyrazine	50 - 1250	6.51	2.27	6.7	6.4	102 (4.2)	101 (11)
N,*N*-Dimethylformamide	150 - 3750	3.00	1.49	23.1	19.0	101 (13)	101 (7.6)
1-Hexanol	150 - 3750	3.46	1.98	41.1	56.6	101 (5.3)	100 (5.7)
3-Octanol	150 - 3750	4.15	1.69	9.1	32.3	102 (1.3)	100 (8.9)
2-Hexen-1-ol	150 - 3750	4.20	2.01	27.8	37.4	102 (1.0)	101 (8.5)
2-Acetylfuran	50 - 1250	7.12	2.07	8.5	11.6	101 (3.0)	100 (10)
Benzaldehyde	50 - 1250	4.62	0.840	19.4	301.9	99.3 (4.4)	93.7 (5.8)
Pentanoic acid	100 - 2500	0.616	0.326	101.8	72.2	101 (18)	100 (6.2)
N,*N*-Dibutylformamide	150 - 3750	1.09	0.596	182.0	107.4	102 (2.4)	101 (4.7)

Hexanoic acid	100 - 2500	0.258	0.215	283.8	77.2	101 (44)	101 (4.1)
Benzyl alcohol	50 -1250	2.62	1.64	37.7	28.2	101 (7.8)	100 (14)
Phenylethyl alcohol	150 - 3750	2.23	1.50	149.8	103.6	101 (5.7)	100 (2.9)

[a] Limit of detection, calculated as the concentration corresponding to 3 times the signal-to-noise ratio.
[b] Relative recovery for a spiked level of 3750 ng/vial for alcohols and formamides, 2500 ng/vial for acids and 1250 ng/vial for all the other standards.
[c] Relative standard deviation

Table 2

Chromatographic and molecular data of the analytes under study.

Peak Number	Compound Name	[1]RT (s)[a]	[2]RT (s)[b]	LRI[c]	Chemical Structure	Chemical Family	Molecular Formula	Log P[d]	VP (mm Hg)[e]	BP (°C)[f]
1	Butanoic acid, ethyl ester	228	0.750	978	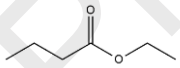	Ester	$C_6H_{12}O_2$	1.3	12.80 (25˚C)	120
2	Dimethyl disulfide	260	0.590	999	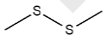	Sulfur-containing	$C_2H_6S_2$	1.8	28.73 (25˚C)	110
3	2,4-Pentanedione	400	0.540	1108	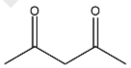	Ketone	$C_5H_8O_2$	0.4	2.96 (20˚C)	138
4	3-Methyl-1-butanol	418	0.490	1119	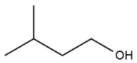	Alcohol	$C_5H_{12}O$	1.2	2.37 (25˚C)	131
5	2,3-Heptanedione	438	0.680	1136	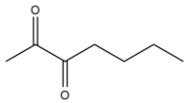	Ketone	$C_7H_{12}O_2$	1.0	3.98 (25˚C)	64

6	3-Octanone	468	0.950	1159	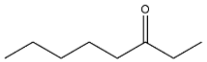	Ketone	$C_8H_{16}O$	2.3	1.50 (25˚C)	170
7	1-Pentanol	472	0.500	1160	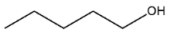	Alcohol	$C_5H_{12}O$	1.6	1.67 (25˚C)	139
8	2,6-Dimethylpyrazine	562	0.620	1232	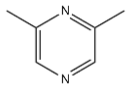	Nitrogen-containing	$C_6H_8N_2$	0.5	0.31 (25˚C)	154
9	*N*,*N*-Dimethylformamide	572	0.470	1236	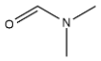	Nitrogen-containing	C_3H_7NO	-1.0	3.87 (25˚C)	153
10	1-Hexanol	604	0.530	1263	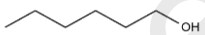	Alcohol	$C_6H_{14}O$	2.0	0.93 (25˚C)	158
11	3-Octanol	654	0.680	1302	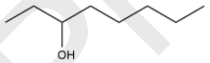	Alcohol	$C_8H_{18}O$	2.8	0.51 (25˚C)	175
12	2-Hexen-1-ol	672	0.490	1317	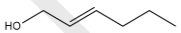	Alcohol	$C_6H_{12}O$	1.4	0.87 (25˚C)	158
13	2-Acetylfuran	794	0.480	1415	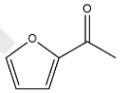	Furan	$C_6H_6O_2$	0.5	0.77 (25˚C)	183
14	Benzaldehyde	810	0.520	1429	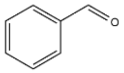	Aldehyde (aromatic)	C_7H_6O	1.5	1.27 (25˚C)	179
15	Pentanoic acid	1086	0.400	1671	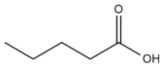	Carboxylic acid	$C_5H_{10}O_2$	1.4	0.45 (25˚C)	185

16	*N,N*-Dibutylformamide	1094	0.750	1677	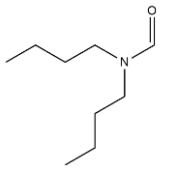	Nitrogen-containing	$C_9H_{19}NO$	2.2	<1 (20˚C)	120
17	Hexanoic acid	1202	0.420	1777	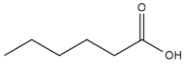	Carboxylic acid	$C_6H_{12}O_2$	1.9	1.6 (25˚C)	205
18	Benzyl alcohol	1222	0.440	1793	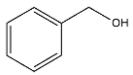	Alcohol (aromatic)	C_7H_8O	1.1	0.09 (25˚C)	205
19	Phenylethyl alcohol	1264	0.490	1831	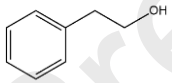	Alcohol (aromatic)	$C_8H_{10}O$	1.4	0.09 (25˚C)	218

[a] Retention time for first dimension
[b] Retention time for second dimension
[c] Linear Retention Index obtained experimentally through the modulated chromatogram
[d] Data obtained from PubChem Database
[e] Vapor pressure, data obtained from The Good Scents Company Information System
[f] Boiling Point, data obtained from ChemSpider Database

Table 2

Characteristics of the four studied SPME sorbent coatings.

Type of coating	**Core type**	**Extraction mechanism**	**Polarity**	**Coating Thickness (µm)**
PA	Fused silica	Absorption	Polar	85
PDMS/DVB	Stableflex	Adsorption	Bipolar	65

DVB/CAR/PDMS	Stableflex	Adsorption	Bipolar	50/30
Zwitterionic PIL	Nitinol	Absorption	Polar	18 ± 6

Table 3
Analytical figures of merit of the HS-SPME/GC×GC-ToFMS methodology after performing matrix-matched calibration of 19 chemical standards.

Analytes	Working Range (ng/vial)	Slope ($\cdot 10^{-4}$)		LOD[a] (ng)		%RR[b] (%RSD[c])	
		PA	PIL	PA	PIL	PA	PIL
Butanoic acid ethyl ester	50 - 1250	9.69	4.96	2.1	2.4	101 (3.4)	101 (17)
Dimethyl disulfide	50 - 1250	9.97	5.08	13.0	4.2	101 (3.6)	100 (6.7)
2,4-Pentanedione	50 - 1250	10.0	7.26	36.7	29.1	101 (13)	100 (5.1)
3-Methyl-1-butanol	150 - 3750	3.33	2.23	61.5	52.3	101 (8.5)	100 (1.6)
2,3-Heptanedione	50 - 1250	2.45	0.723	4.7	5.0	99.1 (8.3)	101 (11)
3-Octanone	50 - 1250	7.06	2.53	9.1	6.6	102 (3.6)	101 (10)
1-Pentanol	150 - 3750	3.35	2.14	56.9	40.5	102 (0.50)	103 (3.1)
2,6-Dimethylpyrazine	50 - 1250	6.51	2.27	6.7	6.4	102 (4.2)	101 (11)
N,*N*-Dimethylformamide	150 - 3750	3.00	1.49	23.1	19.0	101 (13)	101 (7.6)
1-Hexanol	150 - 3750	3.46	1.98	41.1	56.6	101 (5.3)	100 (5.7)
3-Octanol	150 - 3750	4.15	1.69	9.1	32.3	102 (1.3)	100 (8.9)
2-Hexen-1-ol	150 - 3750	4.20	2.01	27.8	37.4	102 (1.0)	101 (8.5)
2-Acetylfuran	50 - 1250	7.12	2.07	8.5	11.6	101 (3.0)	100 (10)

Benzaldehyde	50 - 1250	4.62	0.840	19.4	301.9	99.3 (4.4)	93.7 (5.8)
Pentanoic acid	100 - 2500	0.616	0.326	101.8	72.2	101 (18)	100 (6.2)
N,*N*-Dibutylformamide	150 - 3750	1.09	0.596	182.0	107.4	102 (2.4)	101 (4.7)
Hexanoic acid	100 - 2500	0.258	0.215	283.8	77.2	101 (44)	101 (4.1)
Benzyl alcohol	50 -1250	2.62	1.64	37.7	28.2	101 (7.8)	100 (14)
Phenylethyl alcohol	150 - 3750	2.23	1.50	149.8	103.6	101 (5.7)	100 (2.9)

[a] Limit of detection, calculated as the concentration corresponding to 3 times the signal-to-noise ratio.
[b] Relative recovery for a spiked level of 3750 ng/vial for alcohols and formamides, 2500 ng/vial for acids and 1250 ng/vial for all the other standards.
[c] Relative standard deviation

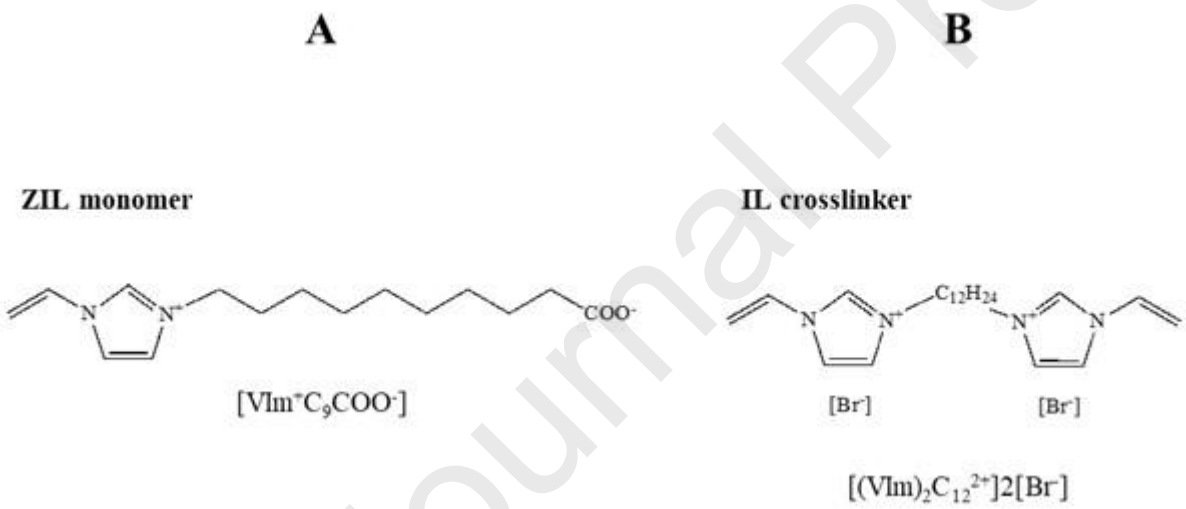

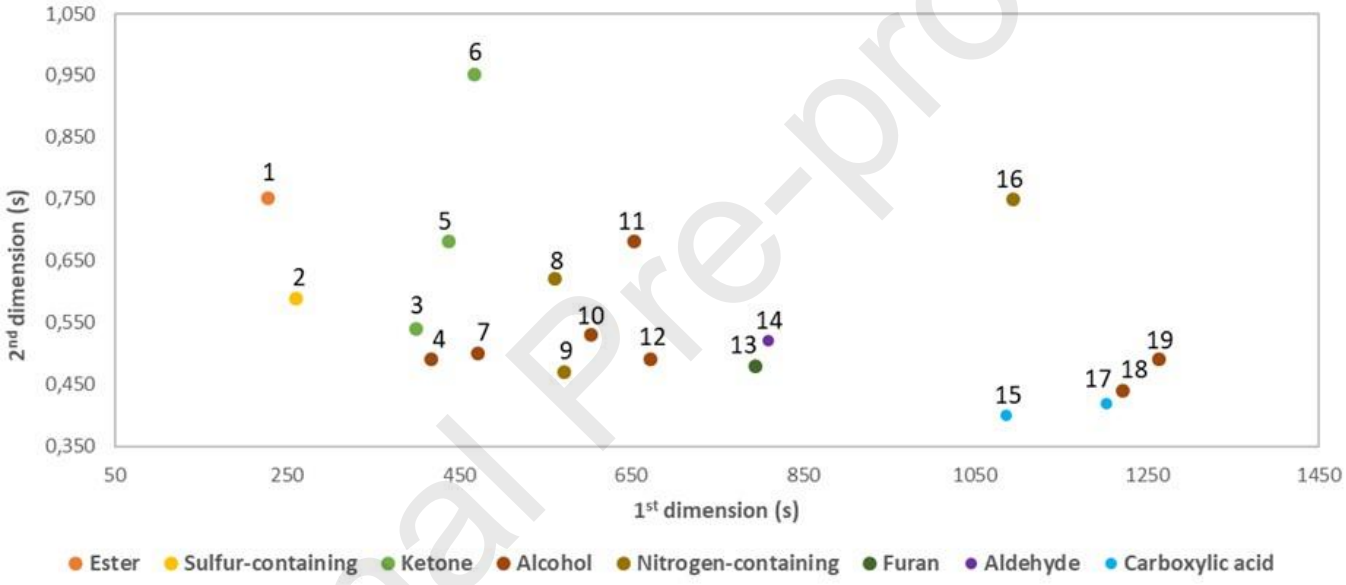

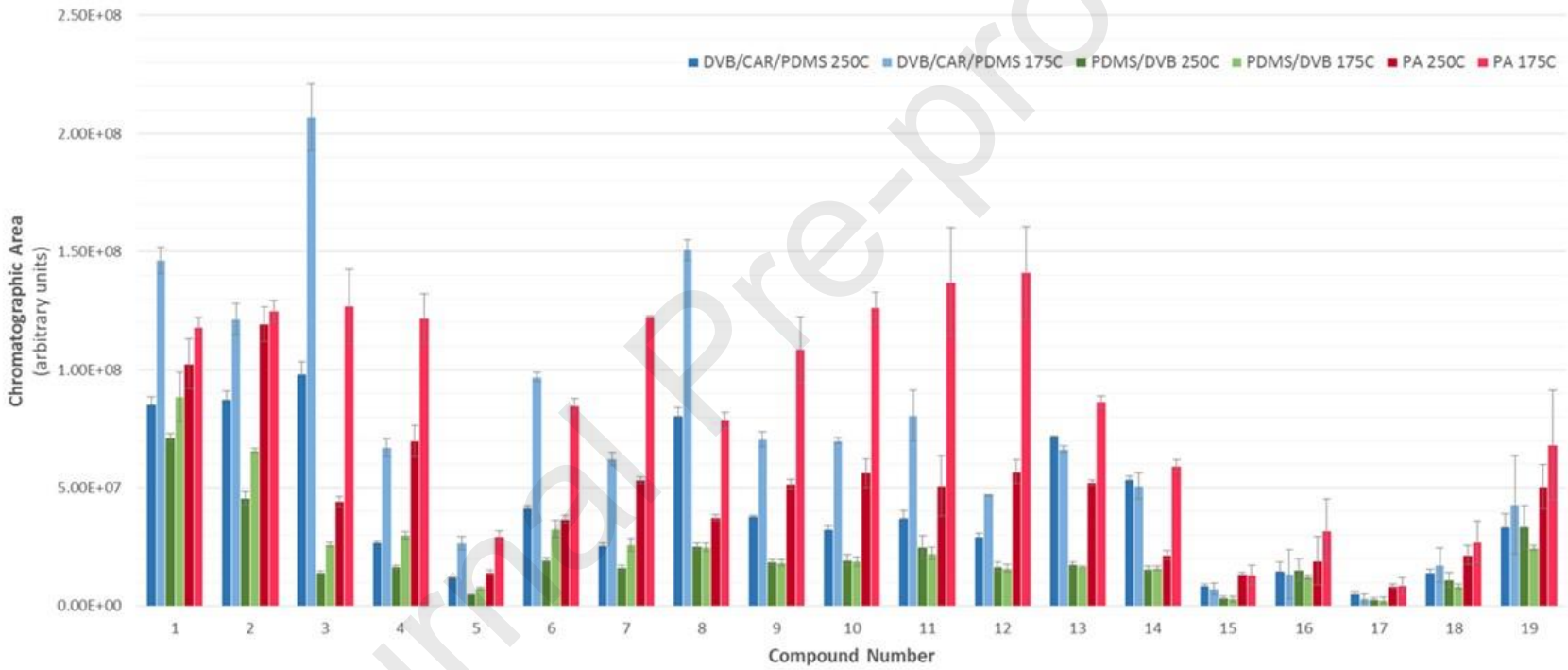

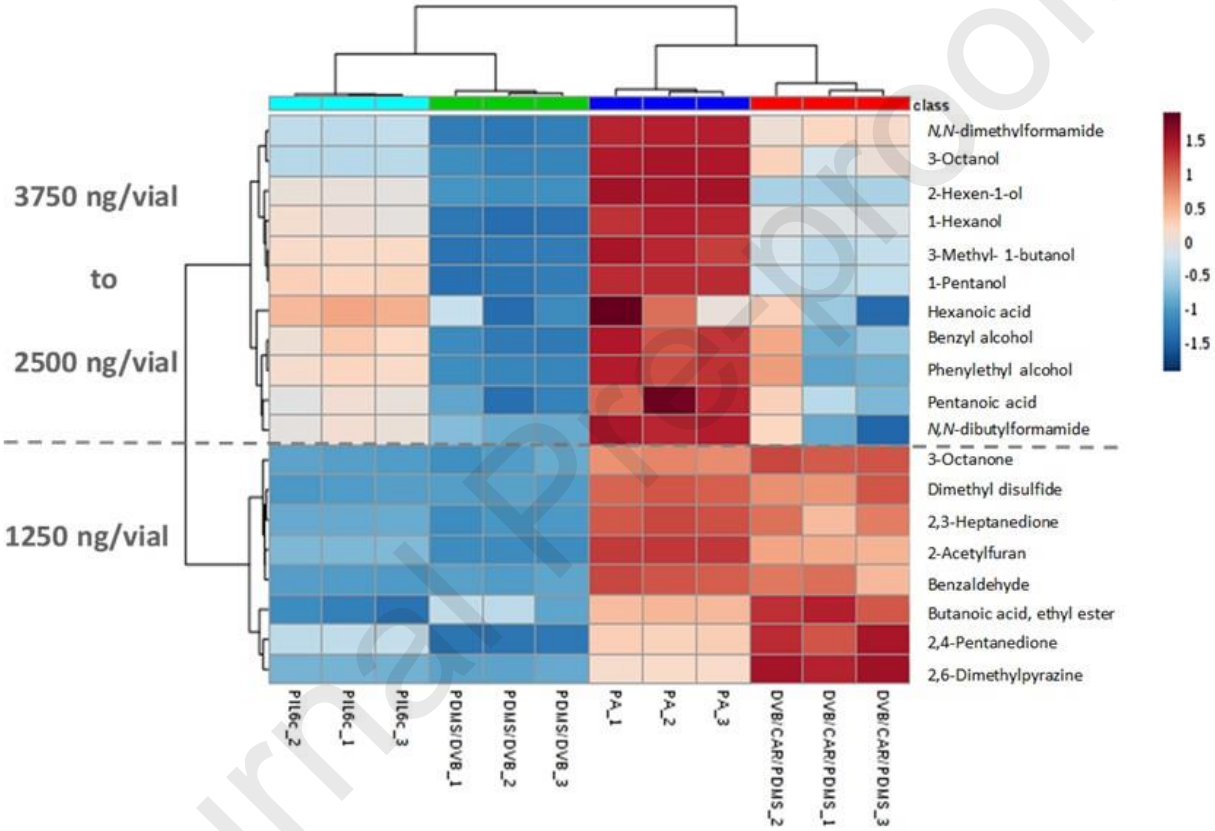

Declaration of Competing Interests

The authors declare that they have no known competing financial interests or personal relationships that could have appeared to influence the work reported in this paper.

Author Statement

Íris R. Carriço: experimental work, validation and formal analysis, writing and editing the final version and preparation of illustrations. **Jéssica Marques**: experimental work, validation and formal analysis, and preparation of illustrations. **Maria J. Trujillo-Rodriguez**: writing, review and editing the final version. **Jared L. Anderson**: responsible for conceptualization, review and editing the final version, supervision and funding acquisition. **Sílvia M. Rocha**: responsible for conceptualization, writing, review and editing the final version, supervision and funding acquisition. All authors read, reviewed, and accepted the final manuscript.

Highlights

- HS-SPME/GC×GC–ToFMS was used for determination of polar death-related VOCs
- First use of zwitterionic polymeric ionic liquids (PIL) for extraction of polar VOCs
- Coatings' extraction efficiency has the following order: PDMS/DVB<PIL<PA<DVB/CAR/PDMS
- PA and PIL provided a good balance representativeness of headspace composition/extraction efficiency
- The 19 polar VOCs were capture from headspace and determined at ng level